

0029-8018(94)00019-0

ARTIFICIAL UPWELLING IN REGULAR AND RANDOM WAVES

Clark C. K. Liu and Qiao Jin

Department of Civil Engineering, University of Hawaii, Honolulu, HI 96822, U.S.A.

(Received for publication 5 August 1994)

Abstract—Mathematical modeling conducted in this study evaluated the hydrodynamic performance of a wave-driven artificial upwelling device in ocean waves off the Hawaiian islands. The device consisted of a buoy (4.0 m in diameter) and a tail pipe (1.2 m in diameter, 300 m in length) with a flow controlling valve. Random ocean waves off the Hawaiian islands used in the device's modeling analysis were synthesized from a wave spectrum obtained from available data. For comparison, the device's performance was also evaluated in regular waves whose height and period are the same as the significant wave height and wave period of random Hawaiian waves. Modeling results indicated that an upwelling flow of 0.95 m³/sec can be generated by this device in random Hawaiian waves and an upwelling flow rate of 0.45 m³/sec can be generated in regular waves. A simple mathematical model which assumed that the device exactly follows the incident waves was used in previous studies. Analysis results also indicated that the simple model cannot satisfactorily simulate the relative velocity and acceleration of the water column in the device. Since the relative velocity and acceleration are important factors in determining the rate of upwelling flow, the simple model must be applied with caution.

NOMENCLATURE

L	length of the pipe under the still water level
H	length of the pipe above the still water level
U	relative velocity of the flow in the pipe
z	heave of the buoy above still water level
m	mass of the floating system
m_w	mass of the water in the pipe
m_a	added mass of the floating system
b	damping coefficient
β	viscous coefficient due to the movement of the device in ambient water
β'	viscous coefficient due to the movement of water inside the pipe
S_w	water line area
S_p	cross section area of water column
F_e	wave exciting force in vertical direction
ρ	water density
g	gravity acceleration
A	incident wave amplitude
k	wave number
ω	wave frequency
f	wave frequency in Hertz
$H_{1/3}$	significant wave height
$T_{1/3}$	significant wave period.

INTRODUCTION

Upwelling occurs off the west coasts of North America, South America, West Africa and a few other coastal regions where along-shore wind stresses push surface water away from the coast, allowing the deep ocean water to rise. Upwelled water from depths below 300 m is cold, clean and rich in nutrients. While upwelling regions account for only 0.1% of the ocean surface, they yield over 40% of the world's fish catch (Roels *et al.*, 1978). Increasing the population of fish and other marine organisms by artificially upwelling the nutrients in deep ocean water has long been considered a means of enhancing marine fisheries, thereby helping to resolve the problem of world food supply shortages.

Land-based mariculture using nutrient rich water pumped from the ocean depths into man-made enclosures has been in existence for over a decade on an experimental basis (Roels *et al.*, 1978; Toyota *et al.*, 1988) and on a commercial basis at the Natural Energy Laboratory of Hawaii (Daniel, 1984). Higher concentrations of nutrients in the deep ocean water supporting the enhanced growth of fish and other marine organisms has been proven by these ventures. However, ocean-based development has not occurred. The major obstacles to ocean-based mariculture using deep ocean water are the high cost of bringing the deep ocean water to the surface and the difficulty of containing the deep ocean water plume (Liu, Chen and Sun, 1989). This study tried to solve the first problem by developing a cost-effective artificial upwelling device.

Ocean thermal energy conversion (OTEC), a method of generating electricity using the temperature difference between surface and deep water in tropical and subtropical oceans, requires the delivery of large amounts of deep ocean water to the surface. After power generation, this deep ocean water is available for ocean mariculture. However, the commercial application of OTEC has not been realized due to its high capital and operational costs. Thus, open ocean mariculture using deep ocean water, if successful, will enhance the feasibility of OTEC commercialization.

Although artificial upwelling can be induced by utilizing ocean currents or other techniques (Liang *et al.*, 1978), wave-driven artificial upwelling seems to be the most promising choice. Various schemes of ocean wave energy conversion have been proposed (McCormick, 1983). Off the Hawaiian islands, wave energy is abundant and persistent and, thus, provides an especially favorable location for wave-driven artificial upwelling. In waters off the Hawaiian islands, the waves and swells due to typical trade winds alone are found approximately 90–95% of the time during the summer months and 55–65% during the winter season (Homer, 1964). In addition to the long duration, very large fetches allow maximum steady state conditions to develop. The deep water waves off the Hawaiian islands can generally be classified into four categories: trade wind waves, Kona storm waves, Southern Pacific swell and North Pacific swell (Moberly and Chamberlain, 1964). Some results derived by Homer (1964) on Hawaiian waves are presented in Table 1 (Gerritsen, 1978).

A wave-driven artificial upwelling device consisting of a buoy and a vertical long pipe with a flow controlling valve is shown in Fig. 1. The valve is closed when the ocean surface goes up; at this time, the device and the water column inside the pipe are accelerated upward. When the ocean surface comes down, the device is subjected

Table 1. Hawaiian wave parameters

Wave type	Significant wave height (m)	Significant wave period (sec)	Expected % of occurrence
Trade wind waves	1.56	8.63	75.3%
Kona storm waves	1.07	6.18	10.3%
Southern Pacific swell	1.56	13.89	74.0%
North Pacific swell	0.79	13.07	53.0%

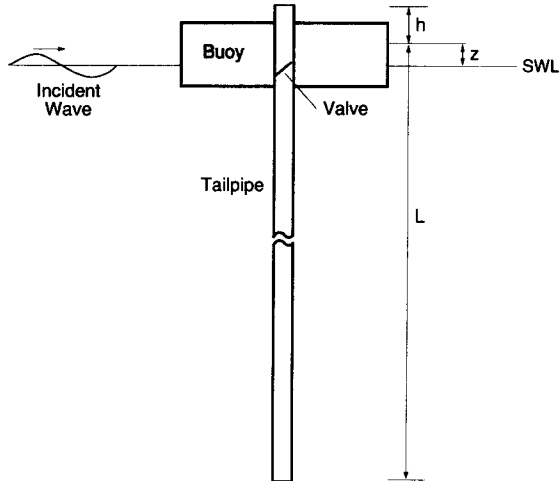


Fig. 1. Schematic diagram of a wave-driven artificial upwelling device.

to a larger inertial force than the water column, which causes the valve to open. The deep ocean water then flows out of the device from the top of its tail pipe.

Wave power was studied intensively by Isaacs and his co-workers (Isaacs and Seymour, 1973; Isaacs *et al.*, 1976; Isaacs, 1979). In their wave pump analysis, a simple mathematical model which assumed that the device exactly follows a sinusoidal ocean surface was used (Isaacs *et al.*, 1976). A more complex model was also formulated by Isaacs *et al.* (1976) by considering the wave-device interaction.

Vershinskiy *et al.* (1987) reported the results of field experiments using a wave-driven artificial upwelling device in the Black Sea. Their field measured upwelling flow rate was higher than that calculated by a mathematical model which was formulated by following the same simplifying assumption of Isaacs *et al.* (1976). Vershinskiy *et al.* (1987) found that their mathematical model underestimated the rate of upwelling flow measured in their field experiments.

Recently, performance of a wave-driven artificial upwelling device which consisted of a buoy with a water chamber, a long tail pipe and two flow controlling valves was evaluated (Chen, Liu and Guo, 1994). The physical modeling of the device was conducted at the Oceanographic Engineering Laboratory of the University of Hawaii. The mathematical model of the device consisted of four simultaneous differential

equations. The first three equations, which describe the motion of upwelled water inside the device, were formulated based on momentum and mass conservation principles. The fourth equation is that of the motion of the device in ambient waves. Both physical and mathematical modeling were conducted in regular sinusoidal waves. Validity of the mathematical model was partially established by comparing calculated time variations of water level in the water chamber with experimental results.

Only wave-driven artificial upwelling in regular waves was investigated in past studies. Actual ocean waves, however, are highly irregular and can be looked at as a superposition of many regular waves. Therefore, a realistic analysis of the performance of a wave-driven artificial upwelling device must consider the randomness of the incident waves. In this study, a time series representing Hawaiian random waves was developed. Two separate analyses of the device's performance were then conducted relative to both regular incident waves and random incident waves. The regular waves used have the wave height and wave period equal to the significant wave height and the significant wave period of Hawaiian random waves.

MATHEMATICAL FORMULATION

When a device as shown in Fig. 1 heaves in the ambient waves, water inside the device keeps moving upward due to inertial forces, bringing the deep ocean water to the surface. This phenomenon can be simulated in terms of equations governing the movement of the water inside the device relative to the device itself. Depending on whether the flow controlling valve is open or closed, two sets of governing equations can be formulated and applied.

When the valve is closed, the water column in the pipe moves with the device. Under this condition, the relative velocity of the water column to the device is zero or,

$$U = 0. \quad (1)$$

The equation of motion of the device takes the following form:

$$(m + m_w) \ddot{z} = -m_a \ddot{z} - b\dot{z} - \beta |\dot{z}| \dot{z} - \rho g S_w z + F_e, \quad (2)$$

where m_w is the mass of the water in the pipe; z is the displacement of the heave of the buoy above still water line; m is the mass of the floating system and F_e is the wave exciting force in the vertical direction.

When the valve is open, the relative acceleration of the water column to the device can be determined by:

$$\dot{U} + \ddot{z} + \frac{z + h}{L + h} \mathbf{g} = 0. \quad (3)$$

The equation of motion of the device then takes the form:

$$m_1 \ddot{z} = -m_a \ddot{z} - b\dot{z} - \beta |\dot{z}| \dot{z} - \beta' U^2 - \rho g S_w z + F_e. \quad (4)$$

Equations (2) and (4) are similar, except that in Equation (2) only the mass of the floating system is considered and in Equation (4) the viscous effect due to relative movement of the water inside the pipe is included.

The added mass m_a , damping coefficient b , and exciting force F_e are important indications of wave and floating body interaction. The rate of flow that a device can upwell is largely determined by values of these parameters. The exciting force indicates the magnitude of the external force acting on the device and is a function of incident waves. The added mass and damping coefficient indicate the extent of resistance and are functions of device design, that is, the dimensions of the device, tail pipe length, etc.

Because the horizontal dimension of the device is much smaller than the wave length, diffraction effects can be ignored and the exciting force F_e is caused mainly by Froude–Krylov force:

$$F_e = C\rho g S_w A \sin(\omega t) , \quad (5)$$

where C is a coefficient.

According to three-dimensional linear wave theory, values of added mass, damping coefficient and exciting force can be determined by integration of velocity potentials over wetted surfaces (Faltinsen and Michelsen, 1974). Details are given in the Appendix.

As part of this study, physical modeling was conducted in a hydraulic laboratory by using a 40:1 scale model. Values of added mass, damping coefficient, and exciting force determined by physical modeling were compared with calculated results from the three-dimensional linear wave theory. The values agree well, especially when wave amplitudes are relatively small (Chen *et al.*, 1994).

Two sets of modeling equations, with known added mass, damping coefficient and exciting force constitute a general mathematical model of wave-driven artificial upwelling. These equations are solved numerically in this study by the Runge–Kutta method.

By assuming the device exactly follows the incident waves, a simple model like the one adopted by Isaacs *et al.* (1976) and Vershinskiy *et al.* (1987) can be formulated. The simple model replaces Equations (2) and (4) in the general model with Equation (6):

$$z = A \sin(\omega t) . \quad (6)$$

DEVICE PERFORMANCE IN REGULAR WAVES

The numerical model was used to evaluate the performance of an artificial upwelling device in regular waves. The device that was evaluated had the following design parameters: mass $m = 12,000$ kg, cross-sectional area of the buoy $S_w = 12.5$ m², length of the tail pipe $L = 300$ m, length of the section above the surface of the water $h = 0.5$ m and cross-sectional area of the tail pipe $S_p = 1.16$ m². Incident waves had height 1.90 m and period 12.0 sec, which are the significant parameters of Hawaiian waves.

Based on the above parameters, added mass m_a , damping coefficient b and coefficient C in the expression of exciting force F_e , calculated based on three-dimensional linear wave theory (see Appendix), are 12,800 kg, 650 kg/sec and 0.97, respectively. Results of mathematical modeling of the movement of the device and the water column inside the device are shown in Figs 2 and 3. The heave of the device followed rather closely that of the incident waves. However, velocities and accelerations of both the device and the water inside the device change in more complex patterns.

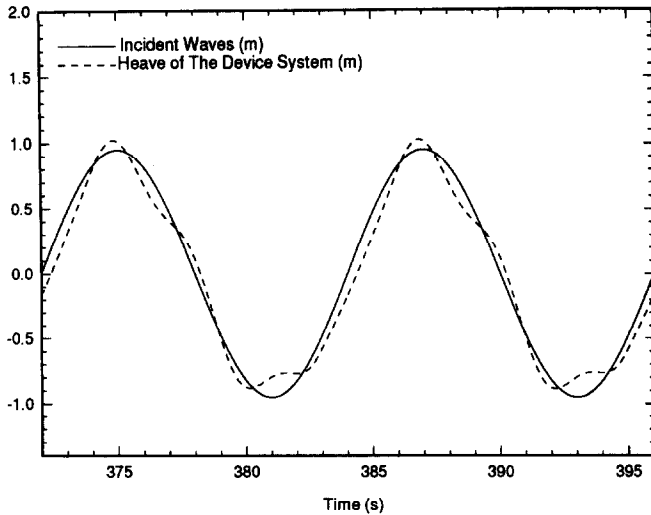


Fig. 2. Heave of the device system in regular waves.

Upwelling flow occurs only when the flow controlling valve is open and the relative velocity of the flow in the pipe (U) is larger than zero. As shown in Fig. 3, the valve will open when the relative acceleration of the water inside the device is larger than zero. The valve will close again when the relative velocity of the water inside the device becomes zero.

Figure 4 gives the simulated results by a simple model assuming the device moves exactly with the incident waves. The amplitude of the acceleration and velocity of the device and the water inside it determine the upwelling flow rate. Therefore, the performance of a device can be evaluated only if the acceleration and velocity can be calculated accurately. From Fig. 2, it can be seen that the pattern of the heave motion of the device system as simulated by our general model was not much different from the motion of the sea surface. Comparison of Figs 3 and 4 show that the amplitude of the velocity and acceleration of the device system as predicted by the general model would be different from those determined by the simple model.

Upwelling flow rate generated by a device can be calculated as a product of the velocity of water inside the device and the cross-sectional area of the tail pipe. Using a time integration of this product over a wave period and then dividing the integration by the period determines an average upwelling flow rate. For the design conditions shown above, the average upwelling flow rate was calculated to be $0.45 \text{ m}^3/\text{sec}$.

Modeling results indicated that the length of the tail pipe has a significant effect on the pumping efficiency of the device; without changing design parameters and wave characteristics, upwelling flow rate increases as the tail pipe becomes longer (Fig. 5). Our mathematical modeling indicated that added mass, damping coefficient and exciting force have no appreciable change as the length of the tail pipe increases. This is verified by results of physical modeling (Chen *et al.*, 1994). However, the mass of the device system increases as the tail pipe lengthens, especially when the flow controlling valve

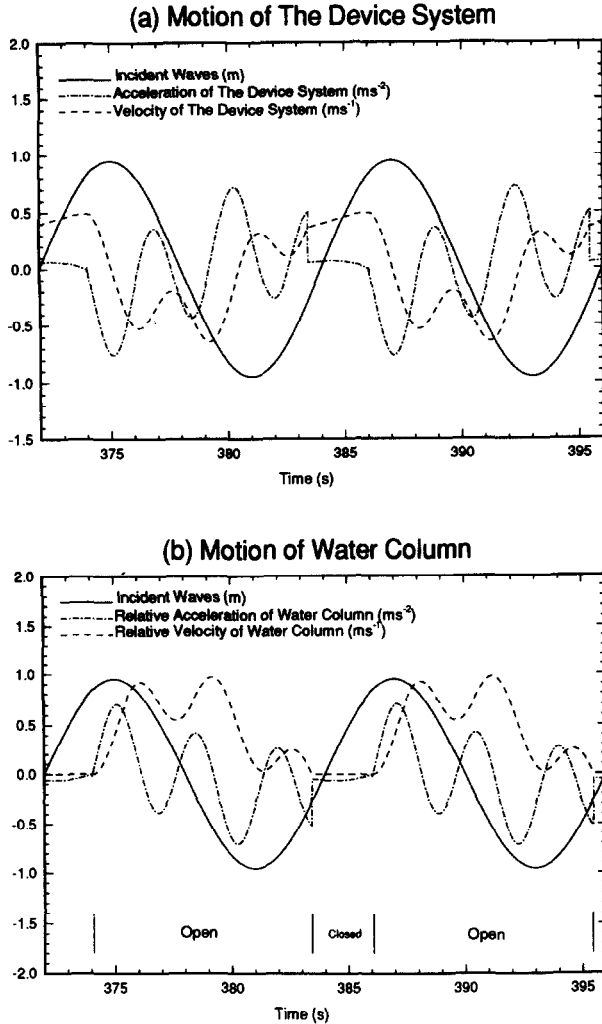


Fig. 3. Motion of the device and the water column in regular waves.

is closed. Therefore, the effect of the length of a tail pipe on the performance of the device probably comes from the change of the mass of the device system. Equation (3) can be looked at as an oscillation equation in which the frequency is inversely proportional to the square root of total mass. As the mass increases, the frequency would decrease and approach that of the incident waves, enhancing the movement of the upwelling device in ambient waves.

Upwelling flow rates generated by the device change with the period of incident waves (Fig. 6). The natural period of the device can be calculated based on its restoration force and total mass. When the valve is closed the total mass includes the mass of the device and of the water column inside it. Under design conditions, the

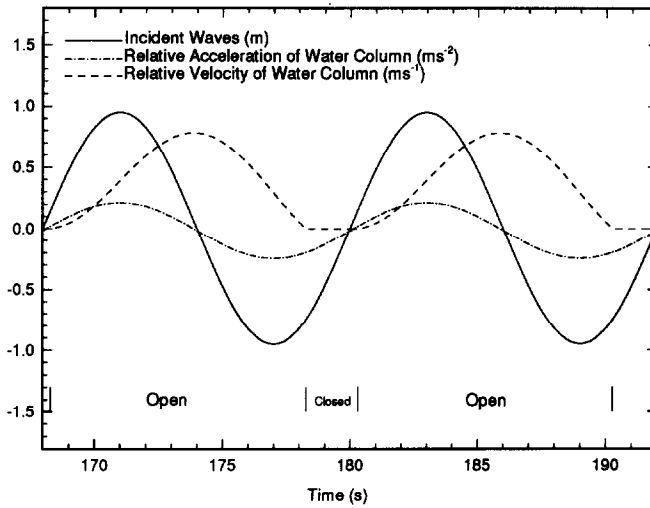


Fig. 4. Motion of the water column simulated by the simple model.

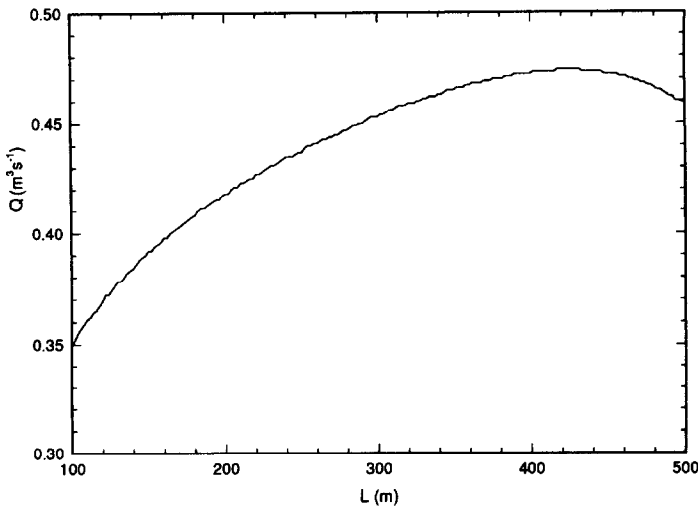


Fig. 5. Effect of tail pipe length on upwelling flow rate.

natural period of the device, when the valve is closed, is about 10.7 sec. When the valve is open the total mass is only that of the device and the natural period is about 2.0 sec. According to Fig. 6, the upwelling flow rate will be higher if the period of incident waves is closer to the natural period of the device when the valve is open. It is noted that resonance may occur and cause operational problems if the period of incident waves is too close to the natural period of the device.

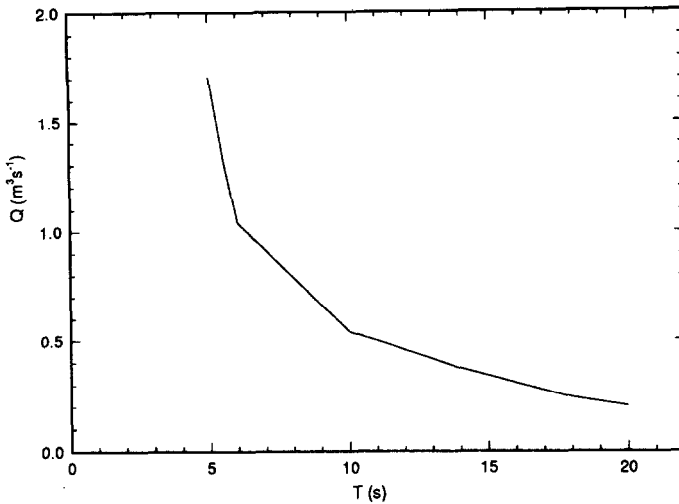


Fig. 6. Wave period and upwelling flow rate.

HAWAIIAN WAVE SPECTRUM AND RANDOM WAVES

Wave frequency and wave height in the ocean are highly irregular and can only be studied by statistical methods. In order to study the performance of a wave-driven artificial upwelling device in actual field conditions in waters off the Hawaiian islands, a time series representing Hawaiian random waves must be developed first and later used in modeling analysis. Usually, this time series can be developed based on an existing wave spectrum. Unfortunately, no wave spectrum characterizing Hawaiian waves is available. In the following, a Hawaiian wave spectrum is synthesized by utilizing available data of Hawaiian wave parameters (Table 1) and the general form of the Bretschneider spectrum.

The Bretschneider spectrum (1959, 1969) is useful to describe random waves when the significant wave height and wave period are known.

$$S(\omega) = 0.1687 H_{1/3}^2 \frac{\omega_{1/3}^4}{\omega^5} e^{-0.675(\omega_{1/3}/\omega)^4}$$

where $\omega_{1/3} = 2\pi/T_{1/3}$. The significant wave period $T_{1/3} = 0.946 T_0$ where T_0 is the peak period. Bretschneider's spectrum is narrow-banded and individual wave heights and wave periods follow the Rayleigh distribution (Chakrabarti, 1987).

Characteristics of the waves off Hawaiian Archipelago are shown in Table 1. A Hawaiian wave spectrum is a superposition of four Bretschneider spectra which describe four typical waves—trade wind waves, Kona storm waves, Southern Pacific swell and North Pacific swell (Fig. 7). From this spectrum, the significant wave height $H_{1/3}$ is about 1.90 m and the significant wave period $T_{1/3}$ is about 12.10 sec. Experiments of OTEC in this area also provide much useful data for the consideration of an artificial upwelling device using wave energy for the ocean-based utilization of deep ocean water (e.g. Noda *et al.*, 1981).

A wave spectrum gives a distribution of wave energy with respect to frequency. It

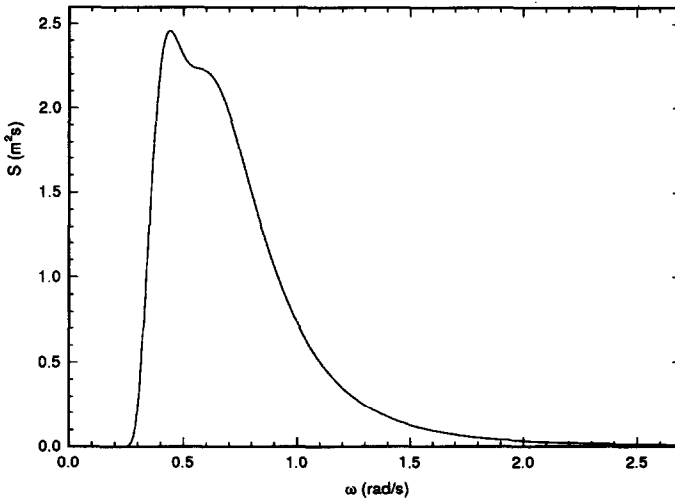


Fig. 7. Spectrum of ocean waves off the Hawaiian islands.

can be decomposed into a number of elements with selected frequency intervals and corresponding energies. Each element can then be represented by a regular wave with specific wave height and period. Random waves can be simulated by a superposition of a series of regular waves. The initial phases of these regular waves are randomly and uniformly distributed in the range of $(0, 2\pi)$. Simulated random waves are shown in Figs 8 and 9.

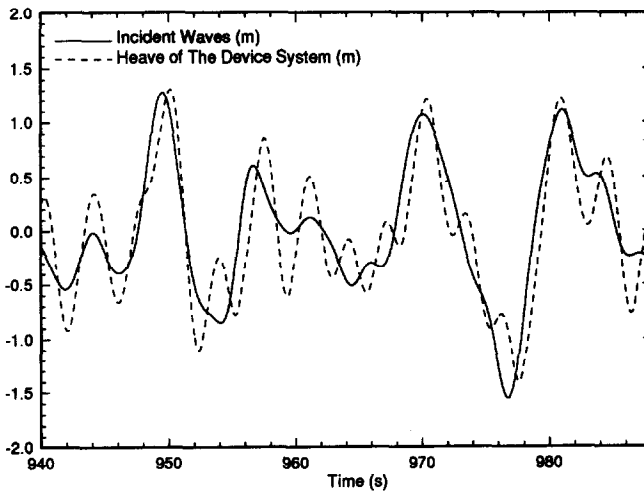


Fig. 8. Heave of the device system in Hawaiian random waves.

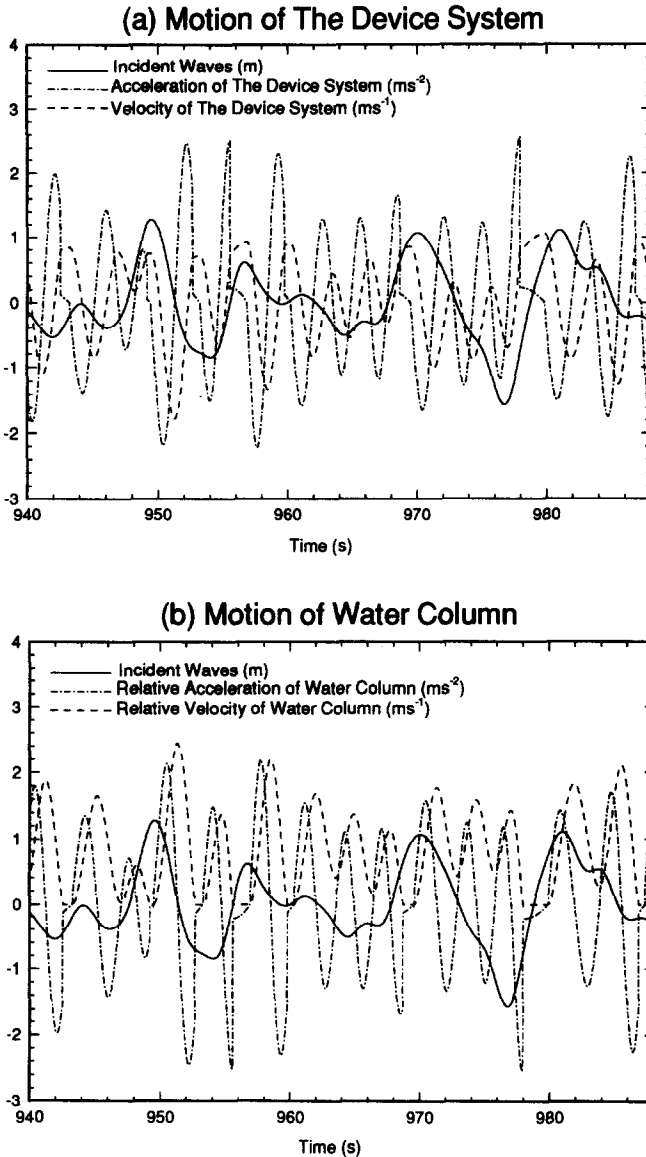


Fig. 9. Motion of the device and the water column in Hawaiian random waves.

DEVICE PERFORMANCE IN RANDOM WAVES

Even if the incident waves are a series of sinusoidal waves, the responses of the artificial upwelling device are not sinusoidal functions because of the valve operation. If the incident waves are irregular, the responses of the artificial upwelling device would be more complicated and interesting.

With the Hawaiian random waves, generated as above, as the model input, movements of the device and the water column inside the device are calculated (Figs 8 and

9). In this computation, added mass and damping coefficient are the averages of individual waves. The exciting force used in the computation is the superposition of exciting forces of individual waves.

The upwelling flow rate is then determined to be $0.95 \text{ m}^3/\text{sec}$. Therefore, the performance of the device is better in random waves than in regular waves with the wave period and height the same as the significant wave period and height of the random waves. Better device performance in random waves can be explained in two ways. First, acceleration of the device in random waves is higher than that of regular waves as indicated by comparing Figs 3 and 9. Second, when the incident wave period approaches the natural period of the device system, the rate of upwelling flow increases significantly (Fig. 6). When random waves with a significant wave period equal that of regular waves, there are components of lower periods in the random waves that tend to produce higher upwelling rates.

Simulation results also indicate that, under the conditions of random waves, the velocity of the water column remains positive most of the time. Therefore, upwelling flow produced by random waves is almost continuous. On the other hand, under the conditions of regular waves, the velocity of the water column is zero for a significant length of the time and therefore the upwelling flow will be intermittent.

CONCLUDING REMARKS

Mathematical modeling was conducted to evaluate the hydrodynamic performance of a wave-driven artificial upwelling device in ocean waves off the Hawaiian islands. The device consisted of a buoy 4.0 m in diameter with a tail pipe of 1.2 m in diameter and 300 m in length. A flow controlling valve was installed in the tail pipe. Random ocean waves off the Hawaiian islands used in the modeling analysis were synthesized from a wave spectrum obtained in this study based on available data. For comparison, the device's performance was also evaluated in regular waves whose height and period were the same as the significant wave height and wave period of random Hawaiian waves.

The mathematical model which simulated the upwelling flow inside the device consisted of two sets of differential equations. One set of equations applies when the controlling valve is closed and the device and the water column inside it move together. Another set of equations applies when the controlling valve is open and the water column moves relative to the device. The interaction of the incident waves, the device and the water column mass is described by model parameters, that is, the added mass, damping coefficient and exciting force. Values of these parameters are determined based on the three-dimensional linear wave theory.

Modeling results indicate that an upwelling flow of $0.95 \text{ m}^3/\text{sec}$ can be generated by this device in random Hawaiian waves and an upwelling flow rate of $0.45 \text{ m}^3/\text{sec}$ can be generated in regular waves. Wave-driven artificial upwelling to bring nutrient rich deep ocean water to the surface is technically feasible, especially for trade wind dominated waters off Hawaiian islands. Results also indicated that past studies, conducted only in regular waves, may have underestimated the efficiency of wave-driven artificial upwelling devices.

In previous studies of wave-driven artificial upwelling, a simple mathematical model was used. It was formulated by assuming the device exactly follows the incident waves.

It was found that the simple model cannot satisfactorily simulate the relative velocity and acceleration of the water column in the device. Because the relative velocity and acceleration are important factors in determining the rate of upwelling flow, the simple model must be applied with caution.

Acknowledgements—This paper is based upon work supported in part by the US National Science Foundation (NSF) under award No. BCS91-11878. Any opinions, findings and conclusions expressed in this publication are those of the authors and do not necessarily reflect the views and policies of the US National Science Foundation.

REFERENCES

- Bretschneider, C.L. 1959. Wave variability and wave spectra for wind-generated gravity waves. Technical Memorandum No. 118, Beach Erosion Board, U.S. Army Corps of Engineers, Washington, D.C.
- Bretschneider, C.L. 1969. Wave forecasting. In *Handbook of Ocean and Under Water Engineering*, Chapter 11. McGraw-Hill, New York.
- Chakrabarti, S.K. 1987. *Hydrodynamics of Offshore Structures*. Computational Mechanics Publications, Southampton.
- Chen, H., Liu, C. and Guo, F. 1994. Hydraulic modeling of wave-driven artificial upwelling. *Proceedings of Oceanology International*, Brighton, U.K., 8–11 March 1994. Spearhead Exhibition, Surrey.
- Daniel, T.H. 1984. OTEC and cold water aquaculture research at the Natural Energy Laboratory of Hawaii. In *Proceedings of PACON '84*, April 1984, pp. MRM 2/47–52. PACON, Honolulu.
- Faltinsen, O.M. and Michelsen, F.C. 1974. Motions of large structures in waves at zero Froude number. In *Proceedings of the International Symposium on the Dynamics of Marine Vehicles and Structures in Waves*, University College, London, pp. 91–106.
- Gerritsen, F. 1978. Beech and surf parameters in Hawaii. Sea Grant Technical Report, UNIHI-SEAGRANT-TR-78-02. Sea Grant College Program, University of Hawaii.
- Homer, P.S. 1964. Characteristics of deep water waves in Oahu area for a typical year, Prepared for the Board of Harbor Commissioners, State of Hawaii. Contract No. 5772. Marine Advisors, La Jolla, California.
- Isaacs, J.D., Castel, D. and Wick, G.L. 1976. Utilization of the energy in ocean waves. *Ocean Engng* 3, 175–187.
- Isaacs, J.D. and Seymour, R.J. 1973. The ocean as a power resource. *Int. Jour. Environ. Studies* 4, 201–205.
- Kajikawa, T. 1991. At-sea experiment on an ocean-based artificial upwelling system. In *Proceedings of Ocean Technologies and Opportunities in the Pacific for the 90's*, Vol. 1, pp. 399–405.
- Liang, N., Huang, P.A., Li, D.J., Chu, L.L. and Wu, C.L. 1978. Artificial upwelling induced by ocean currents—theory and experiment. *Ocean Engng* 5, 83–94.
- Liu, C.C.K., Chen, H.H. and Sun, L.C. 1989. Artificial upwelling and mixing. In *Proceedings of the International Workshop on Artificial Upwelling and Mixing in Coastal Waters*, University of Hawaii, pp. 107–123.
- McCormick, M.E. 1983. Analysis of optimal ocean wave energy conversion. *J. WatWay, Port, Coastal Ocean Engng* 109 (2), 180–198.
- Moberly, R. Jr and Chamberlain, T. 1964. Hawaiian beach system, Prepared for the Harbor Division, Department of Transportation, State of Hawaii. HIG-64-2, Hawaii Institute of Geophysics, University of Hawaii, Honolulu.
- Noda, Edward K., Bienfang, P.K., Kimmerer, W.J. and Walsh, T.W. 1981. Plume survey OTEC-1 mixed-water discharge, JKK Look Laboratory Report, Department of Ocean Engineering, University of Hawaii.
- Roels, O.A., Laurence, M., Farmer, W. and Van Hemelryck, L. 1978. Organic production potential of artificial upwelling marine environment. *Limnol. Oceanogr.* 13, 18–23.
- Toyota, T., Nakashima, T., Ishii, S., Hagiwara, K., Morino, K. and Shimuzu, K. 1988. Design of a deep water supply system for mariculture. In *Proceedings of the Techno-Ocean '88 Symposium*, November 16–18, Kobe, Japan.
- Vershinskiy, N.V., Psenichnyy, B.P. and Solovyev, A.V. 1987. Artificially upwelling the energy of surface waves. *Oceanology* 27(3), 400–402.

APPENDIX

Exciting force, added mass and damping coefficient

Considering the harmonic response of a free floating body under the action of regular waves, the velocity potential can be expressed as:

$$\Phi(x, y, z, t) = \phi(x, y, z) e^{-i\omega t}, \quad (\text{A1})$$

where ω is the angular frequency of the incident waves. The total potential ϕ can be decomposed into:

$$\phi = \phi_I + \phi_D + \phi_R, \quad (\text{A2})$$

where ϕ_I , ϕ_D and ϕ_R are the incident, diffraction and radiation potentials, respectively. The incident potential is the velocity potential of incident waves in the absence of any floating structures. The diffraction potential is the velocity potential caused by the presence of a stationary floating structure in a wave field. The radiation potential is the velocity potential due to the movement of a floating structure in a still water.

The velocity potential and surface elevation of regular incident waves are given as follows:

$$\phi_I = \frac{Ag}{\omega} e^{ikx - kz} \quad (\text{A3})$$

$$\eta = -iA e^{ikx}, \quad (\text{A4})$$

where k is the wave number of the incident waves.

The diffraction and radiation potential can be determined by three-dimensional Green Function Method (Faltinsen and Michelsen, 1974).

The magnitude of the wave exciting force in heave direction, which appears in Equations (2) and (4), can be obtained by taking the real part of the following expression:

$$F_e = i\omega\rho \int_{S_B} (\phi_I + \phi_D) n_z ds = F_I + F_D, \quad (\text{A5})$$

where $\text{Re}(F_I e^{-i\omega t})$ is referred to as the Froude-Krylov force which is obtained by assuming the presence of a body does not affect the pressure distribution in the incident waves; and $\text{Re}(F_D e^{-i\omega t})$ is referred to as the diffraction force that accounts for the scattering of the incident waves.

F_I has the following form:

$$F_I = iC\rho g S_w A. \quad (\text{A6})$$

Here C is a dimensionless coefficient. When the dimension of the floating structure is much smaller than wave length, $C = e^{-kD}$. D is the draft of the floating body.

Generally, F_D can be calculated by an integration of the pressure caused by diffraction potential over wetted surface; it can also be determined by Haskind-Hanaoka relations (Faltinsen and Michelsen, 1974).

The added mass and damping coefficients are obtained by the following expressions:

$$m_a = \frac{1}{\omega^2} \text{Re}(T) \quad (\text{A7})$$

$$b = \frac{1}{i\omega} \text{Im}(T), \quad (\text{A8})$$

where T is defined as:

$$T = i\omega\rho \int_{S_B} \phi_R n_z ds. \quad (\text{A9})$$